Applied Catalysis A, General 610 (2021) 117957

Contents lists available at ScienceDirect

Applied Catalysis A, General

journal homepage: www.elsevier.com/locate/apcata

Liquid-phase synthesis of methyl isobutyl ketone over bifunctional heterogeneous catalysts comprising cross-linked perfluorinated sulfonic acid Aquivion polymers and supported Pd nanoparticles

Francesca Liguori [a], Claudio Oldani [b], Laura Capozzoli [a], Nicola Calisi [c], Pierluigi Barbaro [a,*]

[a] Consiglio Nazionale delle Ricerche, Istituto di Chimica dei Composti Organo Metallici, Via Madonna del Piano 10, 50019, Sesto Fiorentino, Firenze, Italy
[b] Solvay Specialty Polymers (Italy) S.p.A., Viale Lombardia 20, 20021, Bollate, Milano, Italy
[c] Università degli studi di Firenze Dipartimento di Ingegneria Industriale, via s. Marta 3, 50139, Firenze, Italy

ARTICLE INFO

Keywords:
Bifunctional catalysts
Methyl isobutyl ketone
Aquivion
Liquid-phase
Perfluorosulfonic acid

ABSTRACT

The solvent-free hydrogenation reaction of acetone over bifunctional heterogeneous catalysts, comprising cross-linked perfluorosulfonic acid (PFSA) resins and supported Pd nanoparticles, was investigated in the liquid phase under batch conditions. A systematic study was performed by analyzing separately the effect of the main reaction parameters on the reaction outputs. Acetone conversion, selectivity and productivity to methyl isobutyl ketone (MIBK) were measured as a function of the reaction temperature, the amount of catalyst, the Pd loading, the H_2 pressure, the reaction time and the cross-linkage of the polymeric support. Reproducible trends were observed that could be explained in terms of properties of the catalyst, conversion path and kinetics. Best compromise results between selectivity (92 %) and productivity (37.0 $mmol_{MIBK}\ g_{cat}^{-1}\ h^{-1}$) at 19.7 % acetone conversion were obtained for the 0.26Pd@X-link-08-PW79 catalyst, based on 0.8 % cross-linked PFSA support and 0.26 % wt Pd content.

1. Introduction

Methyl isobutyl ketone (MIBK) is a chemical largely used as solvent for paints, coatings and inks, as extracting medium in the synthesis of antibiotics and lubricants, as intermediate in the production of epoxy, acrylic and vinyl resins, as well as a flavouring agent and in food-contact packaging products [1,2]. The current global demand of MIBK exceeds 300 kton y^{-1}, with an expected Compound Annual Growth Rate of 7.5 % over the period 2016–2024 [3,4].

The manufacture processes of MIBK involve three consecutive reaction steps, using acetone (ACE) as starting material: acid or base-mediated aldol condensation of ACE to diacetone alcohol (DAA), acid-catalysed dehydration of DAA to mesityl oxide (MSO), metal-catalysed selective hydrogenation of MSO to MIBK (Scheme 1, path A) [5]. The conventional procedure generates large amount of waste and it is economically and technically unfavourable, due to the use of multiple reactors and processing units.

Heterogeneous *truly bifunctional metal / acid catalysts*, i.e. "a combination of well-defined supported acid and metal sites acting under the same reaction conditions", namely *metals onto solid acids*, are an useful tool to achieve reaction sequences in cascade, in one-pot and in one-stage [6,7]. They are a valuable and eco-friendly option for the production of MIBK, being able to promote the direct conversion of acetone to MIBK over separable and reusable catalysts, combining condensation and hydrogenation steps. A number of heterogeneous bifunctional catalysts have been reported for the synthesis of MIBK [8,9], including patented [10–15] and industrial ones [16]. The usual drawback of this strategy is selectivity. Indeed, under the concurrent conditions of acidic and hydrogenation catalysis, acetone may undergo a very complex reactions network, resulting in a variety of C3, C6, C9 and C12 by-products, due to the several possible condensation, dehydration, isomerisation and hydrogenation side-reactions. A picture of the main potential reactions and products is shown in Scheme 1.

Most of reported bifunctional catalysts have been employed using fixed-bed reactors and streams of gas-phase reagents [17]. However, solvent-free, liquid phase batch processes have also been described, showing higher selectivity to MIBK (up to 90 % at ca. 50 % ACE conversion), under milder reaction conditions (Table S1). In this case, the most convenient catalysts were those based on polymeric supports, particularly sulfonated resins, due to several benefits compared to other

* Corresponding author.
E-mail address: pierluigi.barbaro@iccom.cnr.it (P. Barbaro).

https://doi.org/10.1016/j.apcata.2020.117957
Received 5 October 2020; Received in revised form 18 November 2020; Accepted 2 December 2020
Available online 11 December 2020

materials, including: commercial availability, low cost, easy and tuneable metal loading, high acid density, effective recovery and reuse, good stability, low back pressure evolution, if packed into flow-through reactor systems [18–20]. As expected by the greater affinity for C=C rather than CO= bonds hydrogenation [21,22], palladium was the supported metal of election. By contrast, sulfonated resin-based catalyst suffer from some limitations: catalyst deactivation due to adsorption of the water and diisobutyl ketone (DIBK) produced [23–25], support degradation at high temperatures (> 130 °C) [26], need of relatively high H_2 pressures [27].

In very few instances, liquid-phase operations were performed under continuous flow conditions (Table S2). Compared to batch setups, this adds significant process intensification in terms of increased safety and productivity, simpler downstream processing, smaller hold-up volumes, improved heat transfer and process control [28–30]. Continuous refresh of catalyst may also reduce active sites inhibition [31,32].

We previously reported the use Aquivion® perfluorosulfonic acid resins as effective support for the immobilisation of metal nanoparticles (MNP), and the application of the resulting bifunctional catalysts in the direct conversion of biomass-derived substrates to high added-value chemicals: (-)-menthol and γ-valerolactone [33]. Aquivion® is a family of short side-chain, perfluorinated fluorosulfonic acid polymers (PFSA), produced in a variety of acid densities and featuring acidic strengths comparable to that of sulfuric acid (Hammett acidity ca.−12) [34,35]. Typical of fluoropolymers, they have excellent thermal resistance and chemical inertness, that allow to withstand highly aggressive reaction conditions, including reductive environments [36,37]. Compared to the polymeric congeners Nafion®, Flemion® and Aciplex®, Aquivion® displays a higher crystallinity, ionic conductivity and glass transition temperature (T_g 140 °C) [38]. This has prompted its use as solid acid catalyst in a variety of processes [39–47]. Recently, we described, for the first time, the use of Pt onto an Aquivion cross-linked congener in the catalytic amination reaction of ethyl levulinate to *N*-heptyl-5-methylpyrrolidin-2-one, a bio-derived functional substitute of the REACH-restricted solvent *N*-methyl-2-pyrrolidone [48].

Aim of the present work is the engineering of heterogeneous bifunctional catalysts based on cross-linked Aquivion polymers and their use in the direct synthesis of MIBK from ACE. Investigation of cross-linked derivatives was motivated by the enhanced rigidity and mechanical stability, compared to the uncross-linked (linear) homologues, which facilitates their separation and recovery [49,50]. Herein we report the immobilisation of Pd NP onto cross-linked Aquivion polymers and their application to the one-pot (single reactor unit) and one-stage (reagents and catalyst mixed in a single operation) hydrogenation of acetone, in the liquid phase and under batch conditions. A systematic study was carried out to investigate the effect of catalyst composition and reaction conditions on the reaction outputs. Best compromise conditions were chosen and compared with the literature data.

2. Experimental

2.1. Materials and methods

Unless otherwise stated, all reactions and manipulations were performed under nitrogen using standard Schlenk techniques.

The perfluorosulfonic acid polymers Aquivion® were obtained from Solvay Specialty Polymers Italy, with the following specifications: coarse powders (PW), equivalent weight 794 g mol^{-1} (79)(1.26 mmol $SO_3H \cdot g^{-1}$), CF_3 end-capping group as stabilizer, cross-linkage either 0.0, 0.2, 0.5 or 0.8 wt % (X-link). The labelling scheme adopted refers to these characteristics, i.e. X-link-02-PW79 indicates an Aquivion polymer with the above specification and 0.2 wt% cross-linkage. Typical thermal properties are T_g ca. 140 °C and T_m > 170 °C [35]. The materials were used as received, without further purifications, after sieving to a fraction of size range of 354–500 μm. The choice was motivated by the lower internal mass transfer limitations compared to larger particle sizes [51],

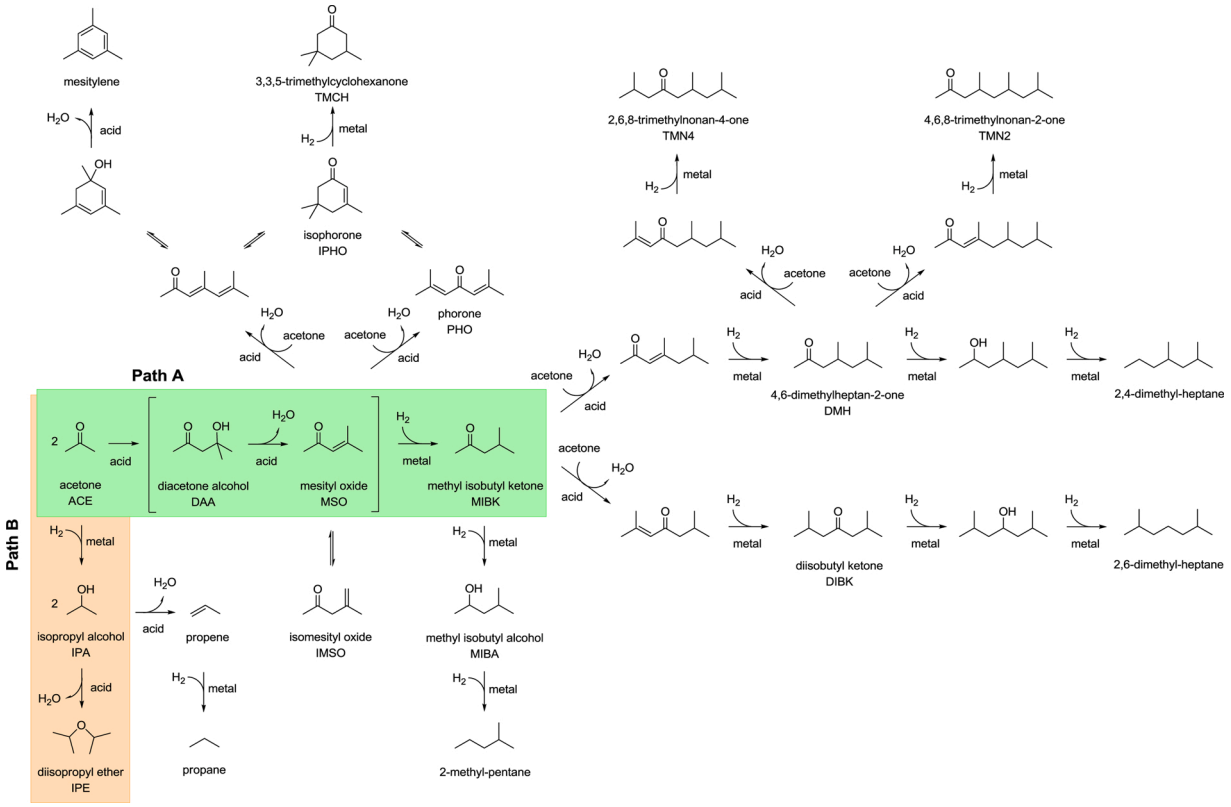

Scheme 1. Potential reaction pathways for the liquid phase conversion of acetone over bifunctional catalysts, under concurrent acid and hydrogenation reaction conditions, with most common products detected.

and by the better sedimentation and easier recovery compared to smaller sizes.

Palladium(II) nitrate trihydrate and acetone ACS reagents (> 99.5 %) were obtained from Aldrich. All other reagents used for calibration curve (methyl isobutyl ketone, methyl-isobutyl alcohol, diisopropyl ether, isopropyl alcohol, diacetone alcohol, mesityl oxide, *iso*-mesityl oxide, 4,6-dimethyl heptan-2-one, diisobutyl ketone, 2,6,8-trimethyl-nonan-4-one) were commercial products and were used as received without further purifications.

The metal content, both in the supported catalyst and leached in the catalytic reaction solutions, was determined by Inductively Coupled Plasma Optical Emission Spectroscopy (ICP-OES) at the Analytical Department of Solvay Specialty Polymers. Typical detection limit for Pd was 0.2 ppm.

TEM (Transmission Electron Microscopy) analyses were performed using a M12 PHILIPS instrument at 120 KeV accelerating voltage. The sample preparation was carried out by dispersing the grinded material into about 1 ml of ethanol and treating the solution in an ultrasonic bath for 30 min. Successively, a drop of solution was deposited onto a carbon coated Cu TEM grid and the solvent left to evaporate. Statistical nanoparticle size distribution analysis was typically carried out on 300–400 particles.

X-ray Photoelectron Spectroscopy (XPS) experiments were carried out in an ultrahigh vacuum (UHV, 10−9 mbar) system equipped with a non-monochromatic X-ray source (Kα radiation, 1486.6 eV) and a hemispherical analyser. The X-ray source was set to work at 120 W (12 kV and 10 mA) and the analyser was set at a constant pass energy of 44 eV for the survey analysis and 22 eV for the high-resolution analysis. Spectra were analysed with the dedicated software CasaXPS. The calibration was obtained using the aliphatic component of carbon 1 s transition (284.8 eV) and the background was subtracted using the Shirley's method.

SEM (Scanning Electron Microscopy) experiments were carried out using a Dual Beam, TESCAN GAIA3 FIB/SEM ultrahigh resolution field emission microscope at 5 KeV voltage. Energy Dispersive X-ray Spectrometry (EDS) experiments, either maps or point-to-point analyses, were acquired on the same instrument at different sample depths.

Swelling measurements. The acetone uptake ability of the catalysts was investigated by measuring their weight change after solvent absorption [52]. Phenex centrifuge tube filters, consisting of a PP filter insert with a PTFE membrane (pore size 0.45 μm) and an outer PP centrifuge tube, were used in the procedure. In a typical experiment, the empty filter insert was weighed, filled with a fixed amount of dry catalyst (about 30 mg) and weighed again to obtain the exact weight of the material (m_i). A small volume of acetone (2 mL) was added to the filter insert at room temperature, that was then sealed using a tethered upper cap and a PTFE lower plug (Fig. S3). After 2 h swelling, he lower plug was removed and the filter insert was assembled in the outer tube and centrifuged (20 min@3000 RPM). After centrifugation, the insert was removed from the outer tube and weighed to obtain the weight of the swollen sample (m_f). The amount of acetone absorbed was then calculated on the basis of the acetone density [$(m_f\text{-}m_i)/d * m_i$], (d =0.791 g/mL) and expressed as mL of acetone per unit weight of material (mL /g).

^{1}H NMR spectra were recorded at 400.13 MHz on a Bruker Avance DRX-400 spectrometer. $^{13}C\{^1H\}$ NMR spectra were recorded at 100.613 MHz on the same instrument using DEPT-135 pulse sequences. Chemical shifts in ppm are relative to tetramethylsilane as external reference.

GC-analyses were performed on a Shimadzu GC 2010 Plus gas chromatograph equipped with flame ionization detector and VF-WAXms (30 m, 0.25 mm ID, 0.25 μm FT) fused silica capillary column. GC–MS analyses were performed on a Shimadzu QP2010S apparatus equipped with the same capillary column.

Reactions under hydrogen pressure and batch conditions were carried out using a stainless steel autoclave (35.3 mL internal volume) constructed at Istituto di Chimica dei Composti OrganoMetallici-CNR (Firenze, Italy) and equipped with a magnetic stirrer, a Teflon® inset and a pressure controller.

The reaction products were unequivocally identified by comparison of the GC retention times, mass spectra and NMR resonances with those of authentic specimens, whenever possible. Quantitative analysis of each reaction product identified was carried out via GC based on calibration curves of pure compounds. Typical coefficient of determination (R^2) parameter for each calibration curve was > 98 %.

2.2. Synthesis of the bifunctional Pd catalysts

The Pd@Aquivion catalysts were prepared using a procedure analogous to that previously described [33]. The synthesis involved two steps: metallation of Aquivion polymers using $Pd(NO_3)_2$ as metal precursor, followed by metal reduction on the metallated polymer using H_2 as reducing agent. All Pd@Aquivion materials were characterized by ICP-OES for metal loading and TEM for Pd nanoparticles (PdNP) size determination. The labelling scheme adopted and the metal loading of each catalyst are summarised in Table 1. Herein, the synthetic procedure is described for X-link-02-PW79 Aquivion material and Pd 1% loading, as representative example.

In a typical experiment, a degassed, brownish solution of $Pd(NO_3)_2$ (40 mg, 0.15 mmol, molar ratio $SO_3H/Pd = 13$) in water (29.0 mL) was added under nitrogen via syringe to a degassed suspension of X-link-02-PW79 (1600 mg) in water (29.0 mL). The mixture was stirred at room temperature for 24 h using an orbital stirrer. After that time, the solution was decanted and the resulting, brown solid material was washed with degassed water (3 × 50 mL). Water (50 mL) was then added under nitrogen and H_2 was bubbled through the suspension at 1 bar for 4 h with stirring at room temperature. The solid obtained was decanted and washed with degassed water (2 × 25 mL), before being dried under high vacuum at 60 °C overnight. The resulting resin obtained as black powder was stored under nitrogen.

2.3. Catalytic experiments

In a typical experiment, a weighted amount of Aquivion-supported Pd catalyst was loaded into the steel autoclave above described and the system was degassed by three cycles of vacuum/nitrogen. A degassed volume of acetone (6 mL) was transferred under nitrogen via a Teflon tube into the autoclave. Nitrogen was replaced by hydrogen with three cycle of pressurization/depressurization. The autoclave was finally charged with the desired pressure of hydrogen at room temperature, then the reactor was heated up to the selected temperature using oil bath. After stirring for the desired time, the reactor was cooled down to room temperature and depressurized. The recovered reaction suspension was transferred in a centrifuge vials and centrifuged for 30 min at 9500 rpm and 16 °C. The clear solution thus obtained was decanted off from the solid catalyst under a stream of nitrogen. A sample of the reaction solution was analysed by GC and GC MS for product identification and quantification. The recovered solid catalyst was analysed by

Table 1
Pd@Aquivion catalysts synthesized.

Catalyst	Support	Pd loading (wt%)[a]
1.00Pd@PW79	PW79	1.00
0.25Pd@X-link-02-PW79	X-link-02-PW79	0.25
1.04Pd@X-link-02-PW79	X-link-02-PW79	1.04
0.14Pd@X-link-05-PW79	X-link-05-PW79	0.14
0.50Pd@X-link-05-PW79	X-link-05-PW79	0.50
1.00Pd@X-link-05-PW79	X-link-05-PW79	1.00
0.10Pd@X-link-08-PW79	X-link-08-PW79	0.10
0.26Pd@X-link-08-PW79	X-link-08-PW79	0.26
0.50Pd@X-link-08-PW79	X-link-08-PW79	0.50
0.91Pd@X-link-08-PW79	X-link-08-PW79	0.91

[a] From ICP-OES analysis.

TEM. ICP-OES analyses were performed to quantify the metal content, both in the recovered catalyst and leached in the catalytic reaction solutions. For recycling experiments, the solid catalyst recovered from the first cycle was placed into the autoclave and a fresh portion of acetone (6 mL) was added under nitrogen. Nitrogen was replaced by hydrogen with three cycle of pressurization/depressurization. The autoclave was charged with the desired pressure of hydrogen at room temperature, then the reactor was heated up to the selected temperature using oil bath for the second catalytic cycle.

The following formulas were used to calculate the conversion of ACE (X_{ACE}), the yield of product P (Y_P) and the selectivity to product P (S_P):

$$X_{ACE}\ (\%) = \frac{n^S_{ACE} - n^M_{ACE}}{n^S_{ACE}} \cdot 100 = \frac{n^C_{ACE}}{n^S_{ACE}} \cdot 100$$

$$Y_P\ (\%) = \frac{F_P\, n^M_P}{n^S_{ACE}} \cdot 100$$

$$S_P\ (\%) = \frac{Y_P}{X_{ACE}} \cdot 100 = \frac{F_P\, n^M_P}{n^C_{ACE}} \cdot 100$$

where:

n^S_{ACE} = moles of ACE before reaction start

n^M_{ACE} = moles of ACE in the reaction products mixture

$n^C_{ACE} = n^S_{ACE}$ - n^M_{ACE} = moles of ACE converted

n^M_P = moles of compound P in the reaction products mixture

F_P =reaction coefficient for compound P: 1 for monomers (C3, IPA), 2 for dimers (C6, MIBK, DAA, MSO, IMSO, IPE, MIBA), 3 for trimers (C9, DIBK, DMH), 4 for tetramers (C12, TMN4)

In a rough approximation, the molar ratio between H_2 and acetone was calculated based on the volume of ACE used (6 mL) and assuming the moles of H_2 as those contained in the autoclave ceiling at the selected pressure and room temperature.

Under our experimental conditions and within the temperature (100−180 °C) and pressure ranges (10−35 bar) adopted, the ACE molar fraction in the gas phase was reported to be negligible [24].

3. Results and discussion

3.1. Synthesis and characterisation

Heterogeneous, bifunctional palladium / acid catalysts were synthesized based on linear and cross-linked PFSA Aquivion® polymeric supports featuring fixed acid sites density (1.26 mmol $SO_3H \cdot g^{-1}$) and different cross-linking degrees, namely 0.0, 0.2, 0.5 and 0.8 % wt. The structure of the Aquivion materials used is sketched in Scheme 2. The linear polymer is commercially available, whereas the cross-linked congeners are not yet commercial products [53,54]. Typical of low cross-linked functional polymers (i.e. less than 2% wt), all the support materials used have a very low surface area in the dry state (less than 0.3 $m^2\ g^{-1}$), consistent with a non-porous, gel-type structure [55,56]. However, the interior of this polymer class can be made accessible by swelling in appropriate solvents, therefore making swellability a crucial parameter for their application in catalysis [18,57]. Usually, the lower the cross-linkage of functional polymers and the smaller is the pore size and the higher the swelling propensity [58,59]. Swelling tests of linear Aquivion polymers in various solvents were previously carried out by us, showing swelling volume to be inversely proportional to the dielectric constant of the solvent [33].

Strongly acidic sulfonated polymers are known to be excellent materials for the preparation of bifunctional metal / acid catalysts, due to the good mechanical, thermal and chemical stability, tuneable metal loading, atomic level dispersion of the metal precursor, thus allowing for the immobilisation of metal nanoparticles of small size. Stabilisation of MNP onto functional polymers may be favoured by electrostatic effects [60] and, whenever a tridimensional network is created by cross-linking of polymeric chains, a steric stabilization may also be effective [61,62]. A number of reviews are available describing the synthesis, properties and applications of sulfonic resins-based catalysts [18,19,63,64]. Despite of the above benefits, the only commercially available bifunctional catalyst based on sulfonic resins is Amberlyst-CH®, a Pd-containing styrene-divinylbenzene macroreticular copolymer, specifically designed for the synthesis of MIBK and TAME (*tert*-amyl methyl ether) [65,66]. Drawbacks of Amberlyst-type polymers are the reduced mechanical stability, resistance to oxidation and maximum operating temperature (130 °C).

Because of the improved chemical resistance, a number of perfluorosulfonic polymers have been used in catalytic application, above all Nafion® [67], but, to the best of our knowledge and with the exception of Aquivion, none of them in a cross-linked variety. Cross-linkage usually results in a enhanced stability (chemical, mechanical, thermal) and thus in the potential for the synthesis of recoverable solid catalysts [68].

In the present work, Aquivion-supported catalysts with diverse Pd content were prepared. Table 1 summarizes the catalysts synthesized and the labelling scheme adopted. The synthetic procedure was analogous to that previously reported for the preparation of the uncross-linked catalyst congeners: metallation of the polymer via ion-exchange using an appropriate Pd(II) precursor in water, followed by in-situ metal reduction with H_2 [33]. Reduction under 1 bar H_2 and room temperature was possible for the immobilised Pd(II) species [69]. The protocol enables the clean and facile synthesis of heterogeneous, bifunctional materials comprising finely dispersed Pd nanoparticles and Brønsted acid single-sites onto a single catalytic body.

All catalysts synthesized in the present work were characterised in the solid state by a combination of spectroscopic, diffraction and microscopy techniques. ICP-OES analyses showed the bulk Pd content in the finished catalysts to be generally in line with the amount of precursor used, thus indicating a metal uptake in the range 85–99 %.

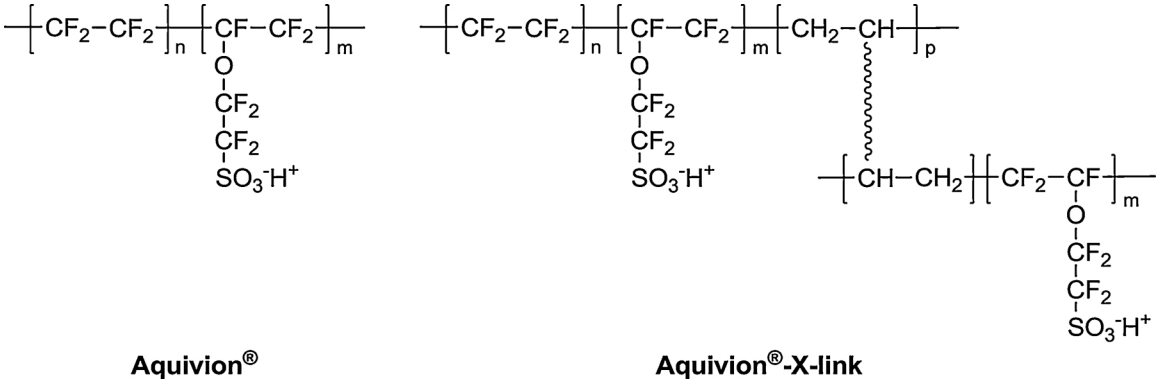

Scheme 2. Schematic representation of the structure of the PFSA Aquivion polymers examined.

Slightly lower uptakes were recorded for higher Pd loadings and cross-linking degrees, that may be tentatively attributed to the worse site-accessibility of the water-soluble Pd ions. XPS experiments were performed to characterise the oxidation state of the supported Pd particles. Irrespective of the Pd loading and the Aquivion support material, XPS spectra indicated the finished catalysts to contain both Pd(0) and Pd(II) species. Thus, the XPS Pd peaks in the 3d region, where the palladium doublet is usually observed, were typically deconvoluted into two oxidation states, Pd(0) around $3d_{5/2}$ 335 eV binding energy and Pd(II) $3d_{5/2}$ around 338 eV [70]. The calculated abundance of the two states was typically around 80 % for Pd(0) and 20 % for Pd(II), respectively. Pd (II) peaks can be attributed to a layer of PdO due to sample manipulation, on the basis of Ar sputtering experiments in agreement with previous findings [33,71], and to oxygen-coordinated species [72,73]. The XPS spectra of 1.04Pd@X-link-02-PW79 and 0.26Pd@X-link-08-PW79 catalysts are reported in Fig. S1, as representative examples, the latter being significantly noisier due to the reduced Pd content. TEM analysis showed all catalysts to contain spheroidal Pd nanoparticles with a broad distribution of diameters centred around 3 nm, sometimes gathered in larger aggregates, with no significant size differences among catalysts. Representative TEM images, size distributions and values are reported in Fig. S2. As previously reported for similar systems, chemisorption experiments were hampered by the limited accessibility of gas reactants to low-cross-linked resin in the dry state [33,69,74]. Swelling properties in acetone were measured for catalysts with comparable metal loading (ca. 1% wt) using a solvent : catalyst weight ratio analogous to that of catalytic experiments (i.e. 6 mL ACE, 100 mg catalyst, vide infra). Swelling volumes ($mL_{ACE}/g_{catalyst}$) are reported in Table 2, showing the ACE uptake to be significantly higher for lower cross-linking degree of the polymeric support material, as expected.

3.2. Catalytic conversion of acetone to MIBK

The as-prepared, bifunctional metal / acid materials were tested as single catalytic body in the solvent-free, direct conversion of acetone to MIBK, in the liquid phase and batch conditions, using H_2 as clean reducing agent. A systematic study was performed examining the effect of the reaction conditions, the diverse supported catalysts and the combination thereof on the process outputs. The performance of the best catalytic system in the range examined was compared with those reported in the literature.

3.2.1. Systematic study

As previously described for other bifunctional batch systems, the selectivity of the catalytic conversion of ACE to MIBK is ruled by the relative kinetics of the several (competitive) potential side-reactions (Scheme 1) [75] Under concurrent hydrogenation and acid catalysis conditions, ACE may undergo two initial reaction paths. Path A, leading to the formation of MIBK, involves a rate determining aldol condensation-dehydration step, which usually requires temperatures > 110 °C, followed by a fast C═C bond hydrogenation. Under these circumstances, DAA and MSO are therefore rarely detected, while the selectivity to MIBK usually decreases with increasing ACE conversion, due to further MIBK condensations reaction [76,77]. Path B involves the hydrogenation reaction of C═O bond to isopropyl alcohol (IPA), eventually followed by further dehydrations. This path is usually kinetically disadvantaged over Pd catalysts, unless high metal loadings, H_2 pressures or low temperatures are used [78,79]. For any given metal / acidic support material combination of the catalyst involved, the critical experimental parameters affecting the rates of above side reactions, hence in turn the MIBK yield, are: i) the reaction temperature, ii) the amount of catalyst (defining the molar ratio between ACE and acidic sites), iii) the loading of supported metal (defining the molar ratio between ACE and hydrogenation sites), iv) the hydrogen pressure (which regulates the molar ratio between H_2 and acetone), v) the reaction time [80].

We have therefore investigated the effect of all the above parameters on the process outputs, either in terms of ACE conversion, selectivity to MIBK, yields of by-products and productivity to MIBK. The catalytic performances were recorded in order to identify the optimal catalyst composition and reaction condition settings. Due to the industrial relevance of the process, which may need to avoid troublesome and costly purification procedures of the reaction mixture [81], priority was given to the maximisation of *MIBK purity and productivity*, rather than the yield of MIBK. Therefore, our best results were selected on the basis of a minumum 90 % selectivity to MIBK. Productivity to MIBK was evaluated in terms of both mmol product per mass of catalyst ($mmol_{MIBK}\ g_{cat}^{-1}\ h^{-1}$) and mol product per mass of noble metal ($mol_{MIBK}\ g_{Pd}^{-1}\ h^{-1}$). Other productivity estimates (e.g. reactor volume productivity, turnover frequency) were used to rationalize the various effects and to compare diverse catalysts, as illustrated in the following sections. In a preliminary investigation, the effect of each parameter was examined separately for each cross-linked support used (see Table 1). Once general trends were established, we compared the performance of the diverse Aquivion catalysts featuring different cross-linkage degrees. Data for the linear, uncross-linked Aquivion resin PW79 catalyst were also recorded for comparison.

Irrespective of the catalyst and the reaction settings used, the only compounds identified in the reaction mixtures at the end of catalytic experiments were ACE, MIBK, DIBK, IPA, DMH and TMN4 (see Scheme 1 for abbreviations). In no case, the total amount of other unidentified products or traces of other chemicals was above 0.06 mol %.

3.2.1.1. Effect of the reaction temperature. Significant acetone conversion to MIBK usually requires relatively high reaction temperatures, due to the slow condensation step. The effect of the temperature was thus examined first, in the range 100–180 °C, in order to evaluate: i) the resistance of the catalysts and ii) the conversion and selectivity to MIBK.

In first set of experiments, fixed amounts of ACE and solid catalyst were mixed at room temperature, then heated under catalytic conditions. After 4 h reaction time, the mixture was cooled down to room temperature and analysed. Whereas all catalysts showed to be insoluble at room temperature, the behaviour of the catalysts recovered after the catalytic runs was remarkably different, depending on the Aquivion support material and the reaction temperature. Upon increasing the temperature, the lower the cross-linkage of the catalyst and the higher was the tendency to form a colloidal dispersion, resulting in unrecoverable gel-type mixtures, irrespective of the Pd loading. Representative findings are summarised in Table 3 for catalysts containing ca. 1 wt% Pd. Thus, for instance, under the conditions of Table 3, the only separable catalysts for reactions performed at 140 °C were those with 0.5 and 0.8 wt % cross-linkage. This finding can be justified by the diverse sol-gel transition temperatures of thermo-responsive polymers depending on their molecular weight (cross-linkage), at a given concentration [82,83]. Acetone, as well as lower alcohols, is a good swelling agent for PFSA in general (see also data in Table 2), hence overswelling with formation of gels is consistently maximised for low cross-linking degrees. It must be pointed out, however, that the findings summarised in Table 3 are valid only within the experimental conditions adopted, i.e. 6 mL ACE and 100 mg catalyst, since catalyst recoverability was significantly affected by

Table 2
Swelling ability of Pd@Aquivion catalysts in acetone.[a].

Catalyst	Swelling volume (mL/g)
1.00Pd@PW79	1.90
1.04Pd@X-link-02-PW79	1.33
1.00Pd@X-link-05-PW79	1.21
0.91Pd@X-link-08-PW79	0.97

[a] Room temperature, ca. 30 mg catalyst in 2 mL ACE.

Table 3
Effect of the reaction temperature on the recovered Aquivion-supported catalysts.[a].

	Temperature (°C)				
Catalyst	100	120	140	160	180
1.00Pd@PW79	separable solid	gel	gel	n.a.	n.a.
1.04Pd@X-link-02-PW79	separable solid	separable solid	gel	gel	n.a.
1.00Pd@X-link-05-PW79	separable solid	separable solid	separable solid	separable solid	separable solid
0.91Pd@X-link-08-PW79	separable solid	separable solid	separable solid	separable solid	separable solid

[a] Reaction conditions: catalyst 100 mg, ACE 6 mL, reaction time 4 h, 25 bar H_2.

the weight ratio ACE / solid catalyst. Upon decreasing this ratio, recoverability worsened for catalysts with lower cross-linking degrees (vide infra). Whenever a catalytic system resulted in an unrecoverable gel, its behaviour was not investigated further.

On the other hand, irrespective of the other parameters, an increase in the reaction temperature led invariably to a higher ACE conversion, but to a lower selectivity to MIBK, due to significant formation of by-products. Representative examples are reported in terms of conversion / selectivity diagrams in Fig. 1, left and Fig. 1, right, for the 1.00Pd@X-link-05-PW79 and 0.91Pd@X-link-08-PW79 catalysts, respectively. Overall, under the conditions range investigated (catalyst amount 100−300 mg, Pd loading 0.1–1.0 % wt, H_2 pressure 10−35 bar, reaction time 2−22 h) ACE conversions were in the range 9–63 % and selectivities to MIBK were in the range 97−63%. Representative data are summarised in Table 4. A larger selection of results is reported in graphical format in the Supporting Information [84].

Upon increasing the reaction temperature, in addition to MIBK, an increase in the formation of DIBK and DMH was mainly observed. This finding indicates that, under the reaction conditions range examined: i) path B - Scheme 1 does not contribute significantly to the conversion of ACE, ii) the acid-catalysed condensation of MIBK with ACE is facilitated at higher temperatures and increasing MIBK concentrations. The composition of the reaction mixture, as a function of the reaction temperature and after 4 h, is graphically reported in Fig. 2 left and Fig. 2 right, for the 1.00Pd@X-link-05-PW79 and 0.91Pd@X-link-08-PW79 catalysts, respectively.

The highest amount of DIBK ever detected in our experiments was around 5 % mol, for reactions performed at temperatures $\geq$ 140 °C, for reaction times > 12 h and using > 100 mg catalyst (see below). The DIBK content was less that 2 % mol, and typically < 1% mol, for reactions performed at temperatures < 140 °C, ≤ 4 h reaction time, irrespective of the catalyst amount.

3.2.1.2. Effect of the catalyst amount. Experiments were performed at increasing amounts of catalyst (100−300 mg) and fixed ACE volumes (6 mL). Since all catalysts feature the same acid density (1.27 mmol $SO_3H \cdot g^{-1}$), this means that the molar ratio between ACE and H^+ sites decreased in this set of experiments, ranging from 650 to 220. Irrespective of the other reaction parameters, an increase in the catalyst amount invariably resulted in a remarkably higher ACE conversion, while selectivity to MIBK was not significantly affected, since yields of both MIBK and condensation by-products increased similarly (at least in the mid-low reaction temperature range). This effect is graphically shown in Figs. 3 and 4for the 0.50Pd@X-link-08-PW79 catalyst, in which selectivity / conversions diagrams and reaction mixtures compositions are reported. This finding is consistent with the fact that the initial acid-catalyzed aldol condensation step, leading to MIBK (Scheme 1, path A), is rate-determining under our experimental conditions. Use of higher amounts of solid catalyst was hampered by the formation of unrecoverable gel-type reaction mixtures, depending on the catalyst cross-linkage and the reaction temperature (see above) [84].

3.2.1.3. Effect of the Pd loading and H_2 pressure. Catalytic experiments were carried out at different H_2 pressures (10−35 bar) or using catalyst with different Pd loadings (0.1–1 % wt), i.e. with increasing densities of hydrogenation sites, showing a much less pronounced effect on the ACE conversion process, compared to the other experimental parameters. Thus, no direct correlation between Pd content and ACE conversion or selectivity to MIBK could be established in our experiments [80]. The conversion / selectivity diagrams obtained for Pd@X-link-08-PW79 catalysts as a function of Pd loading, is reported in Fig. 5, as representative example. Analogously, only a minor increase in ACE conversion and a decrease in MIBK selectivity was observed on doubling the H_2 pressure from 10 to 25 bar, as shown in Fig. 6, left for the 0.91Pd@X-link-08-PW79 catalyst. Significant formation of the hydrogenation by-product IPA (> 1% mol) was only obtained in the instance that a H_2 pressure greater than 25 bar was used, as graphically shown in Fig. 6, right, that justifies for the MIBK selectivity drop observed. These

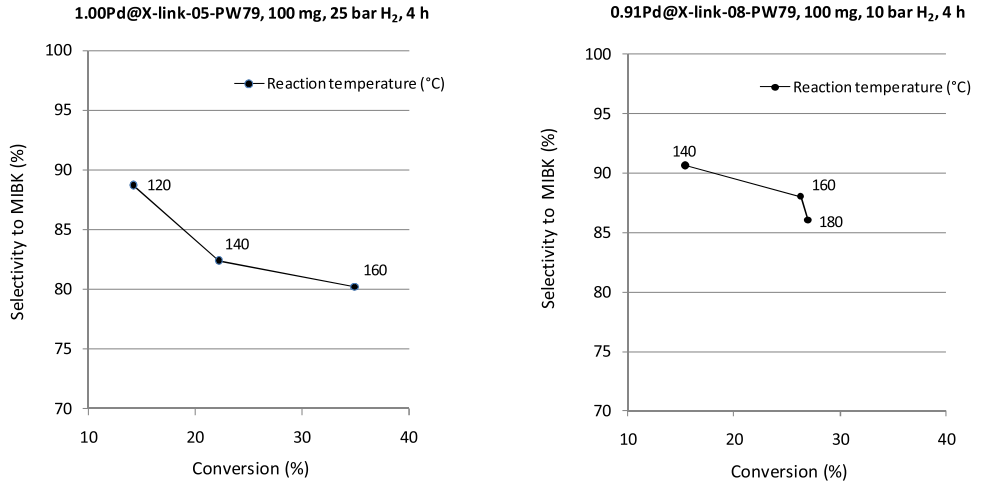

Fig. 1. Conversion / selectivity diagrams, as a function of the reaction temperature, for the hydrogenation reaction of ACE over : left) 1.00Pd@X-link-05-PW79 catalyst (100 mg, 4 h, 25 bar H_2); right) 0.91Pd@X-link-08-PW79 catalyst (100 mg, 4 h, 10 bar H_2).

Table 4
Selected data for the solvent-free, direct synthesis of MIBK from ACE over heterogeneous bifunctional Pd@Aquivion catalysts in the liquid phase and batch conditions.[a].

Entry	Catalyst	Temp. (°C)[b]	H_2 (bar)[c]	Quantity (mg)[d]	Time (h)[e]	Conv. (%)[f]	MIBK		
							Sel.[g] (%)	Productivity[h] (mmol g_{cat}^{-1} h^{-1})	TOF_H[i] (mol mol_H^{-1} h^{-1})
1	1.04Pd@X-link-02-PW79	120	25	100	4	14.7	96.5	29.0	23.0
2	1.00Pd@X-link-05-PW79	120	25	100	4	14.2	88.7	25.7	20.4
3	0.91Pd@X-link-08-PW79	120	25	100	4	11.0	68.7	15.5	12.3
4	1.00Pd@X-link-05-PW79	160	25	100	4	34.9	80.0	57.2	45.4
5	0.14Pd@X-link-05-PW79	160	10	100	4	30.0	85.4	52.3	41.5
6	0.26Pd@X-link-08-PW79	140	10	100	4	19.7	92.0	37.0	29.4
7	0.25Pd@X-link-02-PW79	120	25	200	4	16.5	87.9	14.8	11.8
8	0.10Pd@X-link-08-PW79	140	10	200	2	21.6	84.2	37.1	29.4
9	1.04Pd@X-link-02-PW79	180	25	100	22	63.3	62.8	14.5	11.8

[a] Reaction conditions: ACE 6 mL. Data from GC analysis.
[b] Reaction temperature.
[c] H_2 pressure measured at the reaction onset and room temperature.
[d] Amount of heterogeneous catalyst.
[e] Reaction time.
[f] Acetone conversion.
[g] Selectivity to MIBK.
[h] Productivity to MIBK per weight heterogeneous catalyst.
[i] Turnover frequency per H^+ sites.

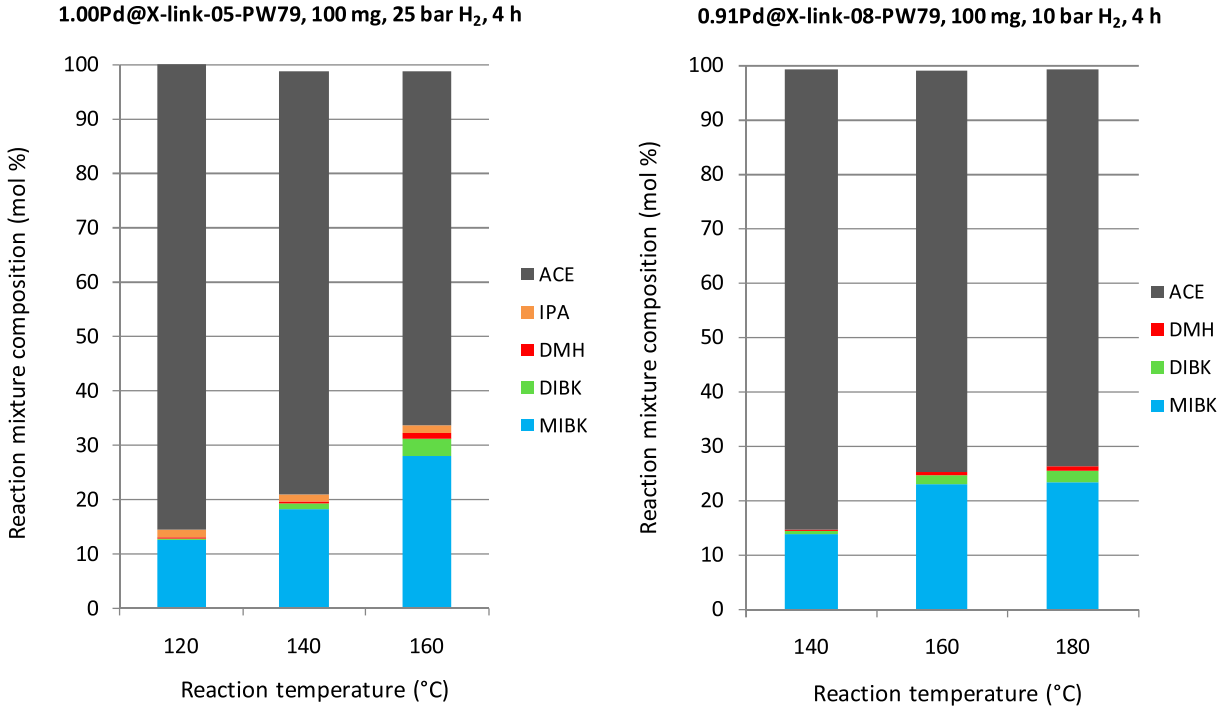

Fig. 2. Reaction mixture composition (mol %), as a function of the reaction temperature, for the hydrogenation reaction of ACE over: left) 1.00Pd@X-link-05-PW79 catalyst (100 mg, 4 h, 25 bar H_2); right) 0.91Pd@X-link-08-PW79 catalyst (100 mg, 4 h, 10 bar H_2).

findings are consistent with our observations above indicating that i) path B in Scheme 1 does not contribute significantly under the experimental conditions adopted and ii) irrespective of the Pd loading, the Pd-catalysed C=C bond hydrogenation step is fast in path A. Indeed, in the hypothesis that the first aldol condensation reaction is rate-determining in the overall two-step process and that hydrogenation is faster, all Pd hydrogenation-related parameters do not significantly affect neither the catalytic performance nor conversion, at least within the experimental ranges examined. Other parameters, such as the number of surface-exposed hydrogenation sites may not pay a role in

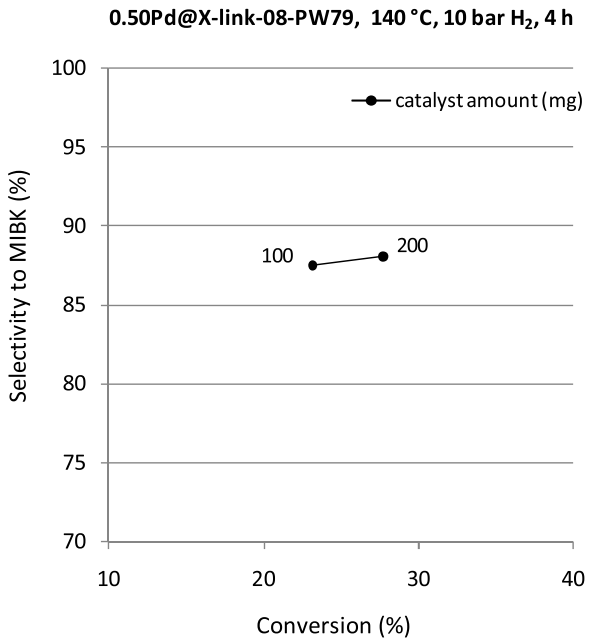

Fig. 3. Conversion / selectivity diagram, as a function of the catalyst amount, for the hydrogenation reaction of ACE over 0.50Pd@X-link-08-PW79 catalyst (140 °C, 4 h, 10 bar H_2).

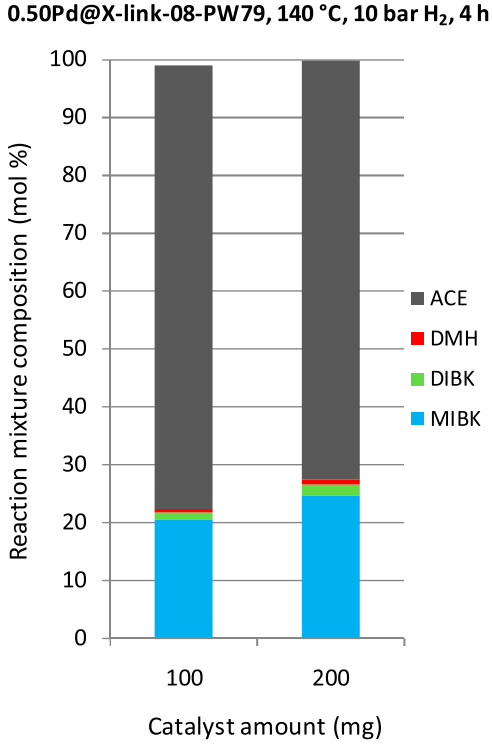

Fig. 4. Reaction mixture composition (mol %), as a function of the catalyst amount, for the hydrogenation reaction of ACE over 0.50Pd@X-link-08-PW79 catalyst (140 °C, 4 h, 10 bar H_2).

this case, given the comparable size of Pd nanoparticles, whereas non-linear dependence of conversion from H_2 pressure may be due site-accessibility and mass transfer phenomena.

It must be underlined that, under our experimental conditions, sub-stoichiometric H_2 / ACE molar ratios were involved throughout, that hampers full conversion of ACE to MIBK in any case, but justifies for the

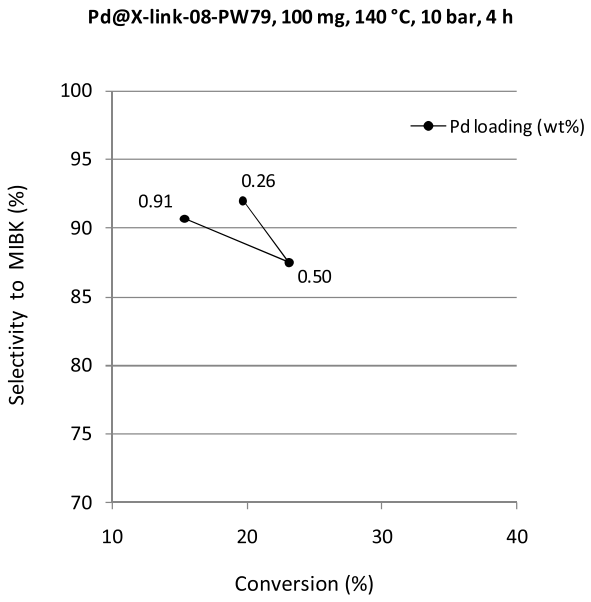

Fig. 5. Conversion / selectivity diagram, as a function of the Pd loading (wt %), for the hydrogenation reaction of ACE over Pd@X-link-08-PW79 catalyst (100 mg, 140 °C 4 h, 10 bar H_2).

negligible hydrogenation of ACE to IPA, in line with previous studies [80]. In all experiments, the amount of H_2 consumed was consistent with that calculated on the basis of the amount of hydrogenation products formed. See Supporting Information.

3.2.1.4. Effect of the reaction time. The effect of the reaction time on the ACE conversion process was drastic. Upon increasing the reaction time from 4 up to 22 h, an increase of conversion (up to 63 %) was associated with a sharp decrease of MIBK selectivity, irrespective of the other experimental conditions. In most cases, this was due to a significant increase of condensation by-products (DIBK, TMN4, DMH), unless a combination of harsh hydrogenation conditions was adopted (i.e. high Pd loading and H_2 pressure), which resulted in the formation of IPA up to 2% mol. Representative examples are reported in Fig. 7 and in Fig. 8 in terms of conversion / selectivity curves and reaction mixture composition, respectively, for the 0.14Pd@X-link-05-PW79 and 0.91Pd@X-link-08-PW79 catalysts.

This effect is safely ascribable to the increase of contact time between the solid acid catalyst and the intermediate conversion product MIBK, which favours the further condensation reaction of MIBK with unconverted ACE. The situation is analogous to that observed in any other catalytic process wherein the desired product is that due to a partial conversion of the substrate, e.g. the partial hydrogenation reaction of alkynes to alkenes [85,86], the hydrogenation of 5-hydroxymethylfurfural to 2,5-bis(hydroxymethyl)furan [87] or the partial hydrogenation of biodiesels [88]. In the present conversion process of ACE, the picture is complicated by the occurrence of coexisting acid-catalyzed condensation and metal-catalyzed hydrogenation reaction conditions.

3.2.1.5. Effect of the catalyst's cross-linking degree. Use of Aquivion support materials with different cross-linking degrees had two main consequence: an effect on the mechanical stability of the solid catalysts and an effect on the catalyst's efficiency.

The effect on the catalyst's stability was discussed above in the relation to effect of the reaction temperature. Catalysts with higher cross-linkage displayed a higher resistance to form colloidal suspensions, hence they were more liable to be recovered in the solid state and reused. This is particularly relevant for practical applications of these catalysts, both in terms of long-term production of MIBK and potential

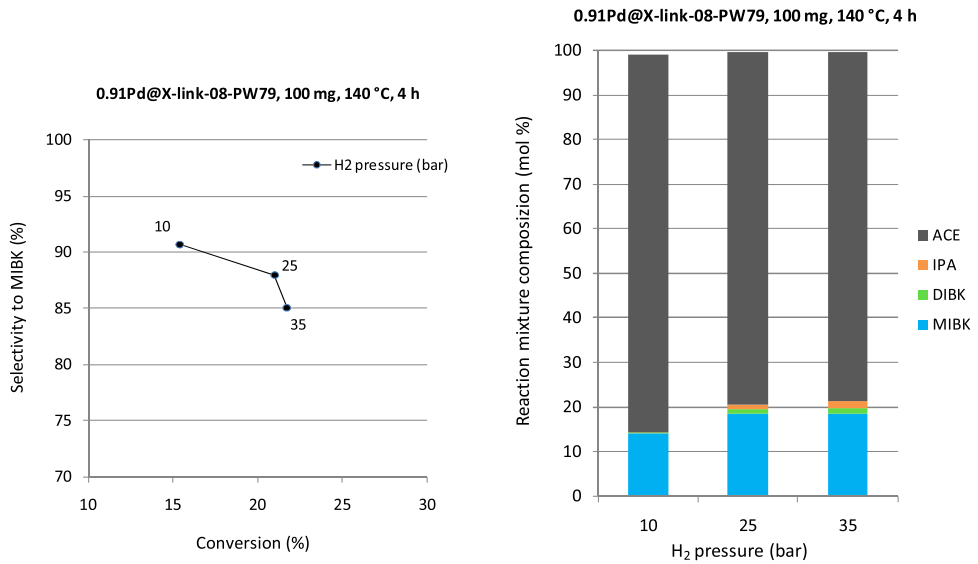

Fig. 6. Hydrogenation reaction of ACE over 0.91Pd@X-link-08-PW79 catalyst (100 mg, 140 °C 4 h), as a function of the H_2 pressure (bar). Left: conversion / selectivity diagram. Right: reaction mixture composition (mol %).

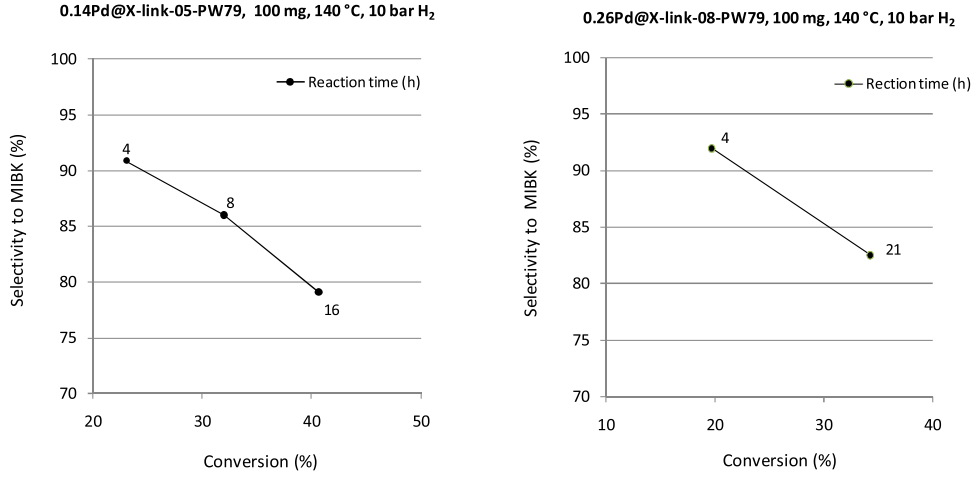

Fig. 7. Conversion / selectivity diagrams, as a function of the reaction time, for the hydrogenation reaction of ACE over: left) 0.14Pd@X-link-05-PW79 catalyst (100 mg, 140 °C, 10 bar H_2); right) 0.91Pd@X-link-08-PW79 catalyst (100 mg, 140 °C, 25 bar H_2).

incorporation into flow-through reactors.

On the other hand, under identical experimental conditions, an increase in the catalyst's cross-linking degree invariably resulted in a lower catalytic activity, as graphically shown in Fig. 9 for catalysts with ca. 1 % Pd loading, as representative example [84][84]. This finding may be attributed to a lower acid sites-accessibility of the substrate upon increase of the cross-linkage of the polymeric support, in agreement with the swelling data of the catalysts in acetone as reported in Table 2. Since the acid-catalyzed condensation step is rate-determining in the overall process, this effect could be quantitatively evaluated by mean of the turnover frequency calculated per H^+ sites ($TOF_H = mol_{MIBK}\, mol_H^{-1}\, h^{-1}$), which indeed decreased in the series 0.2 > 0.5 > 0.8 % cross-linkage, as reported in Table 4, entries 1−3. An analogous result was previously highlighted by us using cross-linked Aquivion polymers in the acid-catalyzed amination reaction of levulinates [48]. Any effect of catalyst's cross-linkage on selectivity shall be considered with care, since selectivity data must be compared at the same conversion level. However, the data available in our hands suggest the lack of any direct correlation in this case.

3.2.2. *General observations*

We performed a systematic study of the ACE conversion process by examining the effects of reaction conditions and catalysts' properties. For each parameter investigated, reproducible trends were observed that can be fully justified in terms of catalysts' features, conversion pathways and reactivity of intermediate products. Despite restricted to a range of experimental conditions, our study revealed that within the ranges explored: i) path B in Scheme 1 is disfavoured, so that the formation of IPA; ii) the aldol condensation step is rate determining; iii) critical experimental parameters for MIBK production are the reaction temperature, the amount of catalyst used and the reaction time, whereas the Pd loading and the H_2 pressure are less important; iv) high selectivity values to MIBK (i.e. > 90 %) are only observed for moderate ACE conversions (i.e. < 30 %). The cross-linkage of the support material has consequences on both catalyst's activity and recoverability. It is clear that optimization of the selective production of MIBK requires a selection of reaction parameters resulting in a very fast aldol condensation reaction of ACE (path A, Scheme 1), thus to maximise the ACE conversion while minimising the contact time with the catalyst, hence the formation of by-products. This suggests that the implementation of a

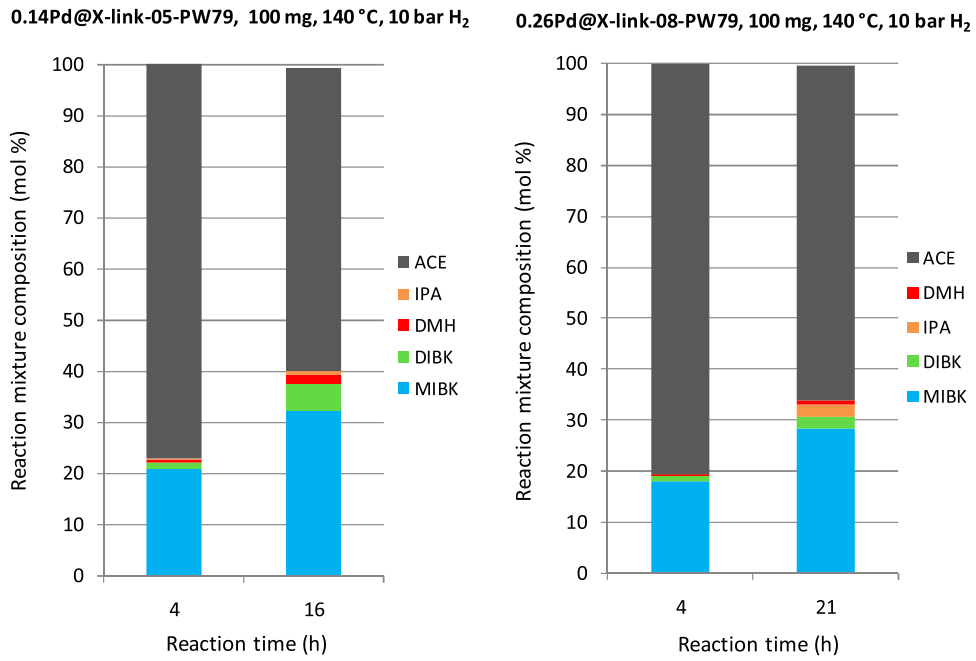

Fig. 8. Reaction mixture composition (mol %), as a function of the reaction time, for the hydrogenation reaction of ACE over: left) 0.14Pd@X-link-05-PW79 catalyst (100 mg, 140 °C, 10 bar H_2); right) 0.91Pd@X-link-08-PW79 catalyst (100 mg, 140 °C, 25 bar H_2).

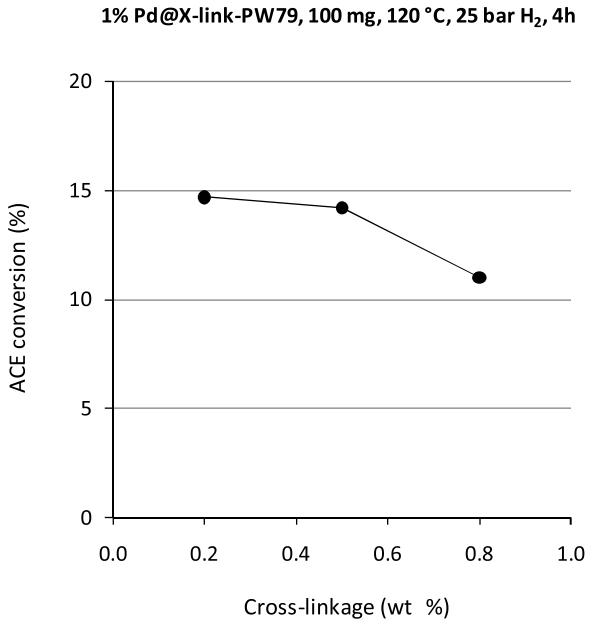

Fig. 9. Conversion dependence from catalyst's cross-linkage for the hydrogenation reaction of ACE over 1.04Pd@X-link-02-PW79, 1.00Pd@X-link-05-PW79 and 0.91Pd@X-link-08-PW79 catalysts (100 mg, 120 °C, 25 bar H_2, 4 h).

continuous flow reactor system may be a promising perspective for the improvement of the present bifunctional catalyst, due to the potential for a careful control of contact time [89]. On the other hand, choice of the best polymeric support for catalyst is ruled by the best compromise solution between catalyst's efficiency and recoverability.

Based on the above observations, the combination of batch experimental parameters and catalyst's properties leading to the best compromise results, yet non-optimised, between catalyst resistance, productivity and selectivity to MIBK were 0.8 cross-linkage of the PFSA support, Pd loading 0.26 %, H_2 pressure 10 bar, reaction temperature 140 °C, catalyst amount 100 mg (catalyst 0.26Pd@X-link-08-PW79). This resulted in a selectivity and a in productivity to MIBK of 92 % and 37.0 $mmol_{MIBK}\ g_{cat}^{-1}\ h^{-1}$, respectively, at 19.7 % ACE conversion, after 4 h reaction time (Table 4, entry 6). The productivity per amount of Pd was 14.3 $mol_{MIBK}\ g_{Pd}^{-1}\ h^{-1}$. It must be mentioned, however, that a higher MIBK selectivity (96.5 %), yet a lower productivity, could be obtained using the 1.04Pd@X-link-02-PW79 catalyst at lower temperature (120 °C) (Table 4, entry 1). Higher productivities around 50 $mmol_{MIBK}\ g_{cat}^{-1}\ h^{-1}$ were obtained in the high temperature range ($\geq$ 160 °C), however with a considerable selectivity drop (ca. 80 %), as above discussed (Table 4, entry 4 and 5).

Importantly, under the conditions above mentioned (see Table 3), the solid catalysts could be easily recovered from the reaction mixture and reused in subsequent ACE hydrogenation cycles, without significant loss of activity or selectivity. As a representative example, the results of first three hydrogenation cycles using the 0.91Pd@X-link-08-PW79 catalyst are reported in graphical format in Fig. 10. In no instance the amount of Pd leached in the catalytic reaction solution was above that of the ICP-OES detection limit. Noteworthy, catalyst reuse was possible even in the upper reaction temperature range (e.g. 160 °C), that can be ascribed to the high thermal stability of the perfluorinated polymeric support. In addition to the ease of separation and recovery, benefits of heterogeneous catalysts, compared to homogeneous systems, may include robustness and stability on the long term. In that case, reuse of heterogeneous catalysts may overcome the usually higher Turnover Numbers typical of homogeneous systems [90]. In the present case, long term experiments over several repetition runs will be conveniently performed once a catalyst showing high selectivity at high conversion level is developed.

3.2.3. *Comparison with literature data*

As above outlined, a number of heterogeneous bifunctional catalysts have been described in the literature for the direct conversion of ACE to MIBK, in the liquid phase and under batch conditions. Data for the most significant examples are summarised in Table 5, whereas a full list is reported in Table S1. Among these catalysts, the only one with industrial application, and by the way the most similar to those herein described, is Amberlyst-CH28 (macroreticular sulfonated resin support, 0.7 wt% Pd), which resulted in a 96 % selectivity to MIBK at 45 % ACE conversion

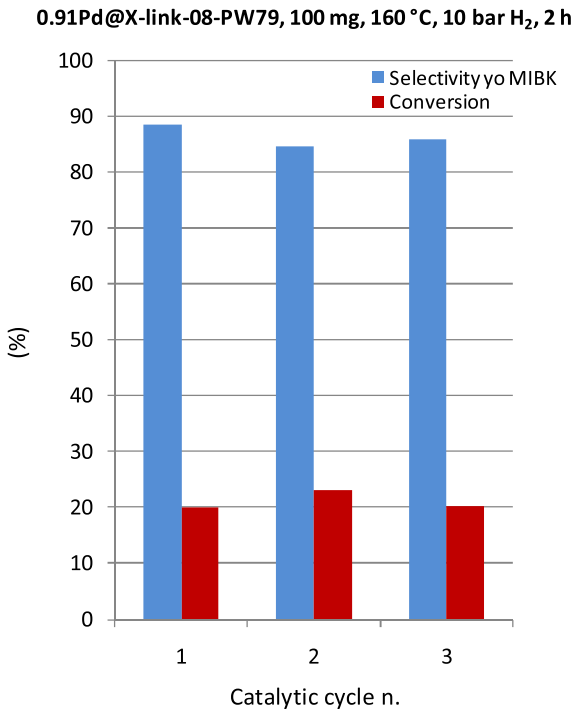

Fig. 10. Catalyst reuse experiments for the hydrogenation reaction of ACE over 0.91Pd@X-link-08-PW79 catalysts (100 mg, 160 °C, 10 bar H_2, 2 h, ACE 6 mL).

(Table 5, entry 4). Various comparative elements with the Aquivion-based catalysts can be highlighted:

i) under very similar reaction conditions (120 °C, 25 bar H_2) the Aquivion catalysts 1.04Pd@X-link-02-PW79 provided a slightly higher selectivity to MIBK (96.5 %), however at a lower conversion value (14.7 %) (Table 5, entry 1). As a consequence, productivities to MIBK were lower for the Aquivion catalyst both in terms of weight catalyst (29.0 vs. 42.4 mmol g_{cat}^{-1} h^{-1}) and weight Pd metal (2.8 vs. 6.0 mol g_{Pd}^{-1} h^{-1}).

ii) best compromise results between catalyst productivity (37.0 mmol g_{cat}^{-1} h^{-1}) and selectivity (92 %) were obtained for the Aquivion catalyst 0.26Pd@X-link-08-PW79, under 140 °C and 10 bar H_2, at 20 % ACE conversion (Table 5, entry 2). In this case, while productivity and selectivity were comparable to those of the Amberlyst system, productivity in terms of noble metal used was much higher (14.3 mol g_{Pd}^{-1} h^{-1}) because of the lower Pd content. This allows for a significant saving of expensive noble metal.

iii) importantly, it must be noticed that in the case of Amberlyst a high conversion was obtained using a remarkable amount of catalyst (5 g, Table S1) that features a high acid-sites density (4.8 mmol $SO_3H \cdot g^{-1}$). This result can be easily justified in terms of low ACE / H^+ sites molar ratio in that case (72) and by the fact that the acid-catalysed aldol condensation step is the rate determining one. Consistently, the Aquivion catalysts, for which a much higher ACE / H^+ ratio can be calculated (649), provide lower ACE conversions under similar reaction conditions. Actually, the normalized parameter TOF_H indicates the Aquivion catalysts to be more active than Amberlyst (23 vs. 8.8 h^{-1}) (Table 5, entry 1 vs. entry 4), that can be attributed to the higher acidic strength and lower cross-linkage of the Aquivion support.

Table 5
Representative literature data for the solvent-free, direct synthesis of MIBK from ACE over heterogeneous bifunctional metal/acid catalysts in the liquid phase and batch conditions.

Entry	Catalyst	Temp. (°C)[a]	H_2 (bar)[b]	ACE/H^+ ratio[c]	Conv. (%)[d]	MIBK				Ref.
						Sel.[e] (%)	Productivity[f] (mmol g_{cat}^{-1} h^{-1})	Productivity[g] (mol g_{Pd}^{-1} h^{-1})	TOF_H[h] (mol mol_H^{-1} h^{-1})	
1	1.04Pd@X-link-02-PW79	120	25	649	14.7	96.5	29.0	2.8	23.0	[i]
2	0.26Pd@X-link-08-PW79	140	10	649	19.7	92.0	37.0	14.3	29.4	[i]
3	0.14Pd@X-link-05-PW79	140	10	649	40.7	79.1	16.5	11.8	13.1	[i]
4	0.7Pd@Amberlyst-CH28	120	30	72	45.0	96.0	42.4	6.0	8.8	[80]
5	0.1Pd@$Cs_{2.5}H_{0.5}PW_{12}O_{40}$	180	7.5	n.a.	42.1	89.8	32.6	32.6	n.a.	[92]
6	0.13Pd@HT[l]	118	27.6	n.a.	38.0	82.2	6.3	4.8	n.a.	[93]
7	0.1Pd@Nb_2O_5/SiO_2	160	20	n.a.	16.6	93.0	165.7	165.7	150.6[m]	[76]
8	0.11Pd@MIL-101	150	7.5	60[n]	59.8	90.2	61.9	56.3	21.5[n]	[94]
9	1.0Pd@Ethane-SiO_2-SO_3H	180	n.a.	148	49.8	82.7	n.a.	n.a.	n.a.	[95]
10	0.1Pd@Mg-Al-mixed-oxide	120	18	n.a.	42.1	88.4	28.9	28.9	n.a.	[96]
11	1.0Pd@Zn-Cr-mixed-oxide	200	5	88[o]	55.6	83.1	39.8	4.0	20.4[o]	[97]
12	0.20Pd@HT-SiO_2[l,p]	190	5	n.a.	16.0	100.0	2135.5	1067.7	n.a.	[79]

[a] Reaction temperature.
[b] H_2 pressure.
[c] Acetone / H^+ sites molar ratio.
[d] Acetone conversion.
[e] Selectivity to MIBK.
[f] Productivity to MIBK per weight heterogeneous catalyst.
[g] Productivity to MIBK per weight Pd.
[h] Turnover frequency per H^+ sites.
[i] This work.
[l] HT = hydrotalcite, amphoteric.
[m] With respect to the total Brønsted + Lewis acidity =1.07 mmol g^{-1}.
[n] With respect to the total Brønsted + Lewis acidity =2.88 mmol g^{-1}.
[o] With respect to the total Brønsted + Lewis acidity =1.95 mmol g^{-1}.
[p] Nano colloidal system.

As above described, use of larger amounts of Aquivion catalysts is hampered by the formation of unrecoverable gel mixtures, however.

iv) reuse of Amberlyst-based catalyst is limited by its upper temperature limit, due to thermal degradation of the resin (130 °C) and by the deactivation of the catalyst, due to the adsorption of water produced during the process that covers the catalytic sites [91]. As a matter of fact, the Amberlyst catalyst could be reused two times, after drying at 80 °C for 3 h after each run [80][80]. By contrast, the Pd-Aquivion catalysts could be efficiently reused with no need of reactivation treatment even at high temperature (160 °C), thanks to the higher thermal stability and hydrophobicity of the perfluorinated matrix.

Other solid catalysts have been reported showing high selectivity to MIBK (> 90 %, Table 5). However, a fair comparison of efficiency should involve similar reaction conditions and ACE conversion levels, which is often hampered by lack of experimental data. In some cases (e.g. entry 5, 9, 11), experiments were performed at high temperatures (≥ 180 °C), whereas a positive contribution of Lewis acid sites onto the catalyst support is arguable (e.g. entry 7, 8, 11). Within these assumptions, the efficiency of the Aquivion-based catalysts is line with that of the reported systems in term of productivity, whereas they ranks high in term of acid sites activity (i.e. TOF_H). It must be underlined, however, that all catalysts (if data are available) were invariably used at much lower ACE / acid sites ratio compared to Aquivion (either using higher amounts of catalysts or acid sites densities), that undoubtedly favours the conversion of ACE, but increase the operating expenses of the process. Very high productivities were reported using an hydrotalcite-supported Pd catalyst, namely 0.20Pd@HT-SiO_2 (Table 5, entry 12), at 190 °C reaction temperature [79]. However, this was a nano-colloidal quasi-homogeneous system, that partially explain for the high activity.

Finally, it must be mentioned that the catalytic synthesis of MIBK from ACE using propan-2-ol as hydrogen transfer agent, instead of hydrogen gas, have been previously reported. Moderate MIBK yields were obtained in gas-phase operations over Cu-Mg-Al catalysts [98,99].

4. Conclusions

We have described the synthesis of heterogeneous bifunctional Pd/acid catalysts, based on a novel class of cross-linked perfluorinated sulfonic acid polymers, and their application to the one-pot, single stage synthesis of MIBK from acetone in the liquid phase. A systematic study was performed analyzing the separate effect of key reaction parameters and catalysts' features on the process outputs. All effects were reproducible and could be rationalized in terms of reaction pathway, kinetics and active sites accessibility. Under our experimental conditions, a mechanism consistent with a first, rate-determining acid-catalysed aldol condensation step, followed by a relatively fast metal-catalysed hydrogenation was demonstrated. Accordingly, the reaction temperature, the reaction time and the molar ratio ACE / H^+ sites showed to be critical in the processes, whereas the Pd-related parameters (i.e. Pd loading, H_2 pressure) had no significant effect on the catalytic performance. The cross-linking degree of the polymeric support showed a positive effect on the catalyst's stability and recoverability, whereas slightly decreased its activity. Non-optimised selection of reaction conditions and catalyst properties resulted in high selectivity to MIBK (up to 96 %) at moderate ACE conversion, wherein remarkable productivity (up to 57 $mol_{MIBK}\ g_{cat}^{-1}\ h^{-1}$) and turnover frequency under mild conditions (140 °C, 10 bar H_2) were attributed to the high acidic strength of the fluorosulfonic acid support. Compared to commercial Amberlyst-CH28, the catalysts herein described offer the unquestionable benefit to be effective at lower Pd loading, hence allowing for the savings of noble metal, whilst affording comparable performance. As product purity decreases upon increasing conversion in the process, best compromise results between selectivity (92 %) and MIBK productivity per unit metal (14.3 $mol_{MIBK}\ g_{Pd}^{-1}\ h^{-1}$) represent a significant outcome of the present catalytic system, that doubles that of the Amberlyst one in term of reduction of precious metal usage. In addition, the present catalyst can be reused with no efficiency decay at high reaction temperature, that can be attributed to the thermal stability of the hydrophobic perfluorinated polymeric support.

The results obtained indicate cross-linked Aquivion type fluorinated polymers to be a promising class of materials for the engineering of truly heterogeneous bifunctional catalysts, targeting multistep reaction processes in one-pot, featuring high efficiency and resistance. Potential applications are several, particularly in the catalytic valorisation of plant biomass [100], wherein cascades of metal / acid - mediated reactions are required for the direct conversion of feed to added-value platform chemicals [101,102]. To the best of our knowledge no other examples have been reported in the literature, nor are commercially available, of cross-linked PFSA materials. Based on the high acid catalysis activity and resistance herein demonstrated, we believe that these materials may represent an extremely useful option to convention sulfonated resins, whose application as catalysts are plenty in several fields at the industrial level [64,103]. As perspective, our findings also suggest the synthesis of PFSA materials with higher cross-linkage (> 1 %) and acid sites density (> 2 $mmol \cdot g^{-1}$) to be key in the design of catalysts with enhanced performance.

CRediT authorship contribution statement

Francesca Liguori: Investigation, Validation, Writing - review & editing. **Claudio Oldani:** Resources, Writing - review & editing. **Laura Capozzoli:** Investigation. **Nicola Calisi:** Investigation. **Pierluigi Barbaro:** Conceptualization, Methodology, Writing - original draft, Writing - review & editing, Supervision.

Declaration of Competing Interest

The authors declare that they have no known competing financial interests or personal relationships that could have appeared to influence the work reported in this paper

Acknowledgments

Thanks are due to Centro Microscopie Elettroniche - Area di Ricerca CNR, Firenze and Sig. Carlo Bartoli (ICCOM-CNR) for technical design and assistance.

Appendix A. Supplementary data

Supplementary material related to this article can be found, in the online version, at doi:https://doi.org/10.1016/j.apcata.2020.117957.

References

[1] E.O. Greiner, K. Yokose, Methyl Isobutyl Ketone (MIBK) and Methyl Isobutyl Carbinol (MIBC). CEH Product Review: Chemical Economics Handbook, SRI International, 2002. August.
[2] W.F. Hoelderich, Stud. Surf. Sci. Catal. 41 (1988) 83–90.
[3] Methyl Isobutyl Ketone Product Information, The Dow Chemical Company, 2002. Form No. 327–00032–0405, June.
[4] www.transparencymarketresearch.com/methyl-isobutyl-ketone.html (accessed June 2020).
[5] Y. Qi, Z. Wang, R. Wang, Appl. Catal. 53 (1989) 63–70.
[6] M.J. Climent, A. Corma, S. Iborra, ChemSusChem 2 (2009) 500–506.
[7] F.X. Felpin, E. Fouquet, ChemSusChem 1 (2008) 718–724.
[8] P. Barbaro, F. Liguori, N. Linares, C. Moreno-Marrodan, Eur. J. Inorg. Chem. (2012) 3807–3823.
[9] M.J. Climent, A. Corma, S. Iborra, Chem. Rev. 111 (2011) 1072–1133.
[10] T. Ushikubo, Y. Kakuno, H. Tsujiura (Mitsubishi Kasei Corporation), Patent No. EP0458216 (A1), 1991.
[11] M. T. Vandersall, R. A. Weinand (Rohm and Haas Company), Patent No. EP1321450 (A2), 2003.
[12] K. Schmitt, J. Disteldorf, W. Flakus, W. Hubel, W. Eickel (Veba-Chemie Aktiengesellchaft), Patent No. US3953517, 1976.
[13] T. J. Huang, W. O. Haag (Mobil Oil Corporation), Patent No. US4339606, 1982.

[14] P. Y. Chen, S. J. Chu, K. C. Wu, W. C. Lin (Industrial Technology Research Institute), Patent No. US5684207A, 1997.
[15] Y. Higashio, T. Nakayama (Sumitomo Chemical Company, Limited), Patent No. EP0227868(A1), 1985.
[16] T. E. Hahn, J. J. Gildenhuys, B. Van Dyk, J. C. Crause, P. Moodliar (Sasol Technology Pty Ltd), Patent No. US222612 (A1), 2010.
[17] Y. Zhou, H. Duan, B. Lin, K. Han, J. Wei, Reac. Kinet. Mech. Cat. 125 (2018) 303–317. Fore a recent example see:.
[18] F. Liguori, C. Moreno-Marrodan, P. Barbaro, Chinese J. Catal. 36 (2015) 1157–1169.
[19] P. Barbaro, F. Liguori, Chem. Rev. 109 (2009) 515–529.
[20] B. Corain, M. Kralik, J. Mol, Catal. A Chem. 159 (2000) 153–162.
[21] P. Meric, K.M.K. Yu, A.T.S. Kong, S.C. Tsang, J. Catal. 237 (2006) 330–336.
[22] P. Gallezot, D. Richard, Catal. Rev. Sci. Eng. 40 (1998) 81–126.
[23] E. du Toit, R. Schwarzer, W. Nicol, Chem. Eng. Sci. 59 (2004) 5545–5550.
[24] E. du Toit, W. Nicol, Appl. Catal. A Gen. 277 (2004) 219–225.
[25] W.K. O'Keefe, F.T.T. Ng, G.L. Rempel, Ind. Eng. Chem. Res. 46 (2007) 716–725.
[26] Y. Román-Leshkov, J.N. Chheda, J.A. Dumesic, Science 312 (2006) 1933–1937.
[27] J.A. Trejo, J. Tate, D. Martenak, F. Huby, S.M. Baxter, A.K. Schultz, R.J. Olsen, Top. Catal. 53 (2010) 1156–1162.
[28] K. Masuda, T. Ichitsuka, N. Koumura, K. Sato, S. Kobayashi, Tetrahedron 74 (2018) 1705–1730.
[29] C. Wiles, P. Watts, Green Chem. 16 (2014) 55–62.
[30] R. Ricciardi, J. Huskens, W. Verboom, ChemSusChem 8 (2015) 2586–2605.
[31] M.B. Plutschack, B. Pieber, K. Gilmore, P.H. Seeberger, Chem. Rev. 117 (2017) 11796–11893.
[32] L. Vaccaro, D. Lanari, A. Marrocchi, G. Strappaveccia, Green Chem. 16 (2014) 3680–3704.
[33] C. Moreno-Marrodan, F. Liguori, P. Barbaro, S. Caporali, L. Merlo, C. Oldani, ChemCatChem 9 (2017) 4256–4267.
[34] V. Arcella, A. Ghielmi, G. Tommasi, Ann. N.Y. Acad. Sci. 984 (2003) 226–244.
[35] www.solvay.com/en/brands/aquivion-pfsa (accessed May 2020).
[36] M. Danilczuk, A.J. Perkowski, S. Schlick, Macromolecules 43 (2010) 3352–3358.
[37] A. Ghielmi, P. Vaccarono, C. Troglia, V. Arcella, J. Power Sources 145 (2005) 108–115.
[38] S. Subianto, M. Pica, M. Casciola, P. Cojocaru, L. Merlo, G. Hards, D.J. Jones, J. Power Sources 233 (2013) 216–230.
[39] L. Bianchi, E. Ballerini, M. Curini, D. Lanari, A. Marrocchi, C. Oldani, L. Vaccaro, ACS Sustainable Chem. Eng. 3 (2015) 1873–1880.
[40] A. Karam, N. Sayoud, K. De Oliveira Vigier, J. Lai, A. Liebens, C. Oldani, F. Jérôme, J. Mol. Cat. A Chem. 422 (2016) 84–88.
[41] H. Shi, Z. Fan, B. Hong, M. Pera-Titus, ChemSusChem 10 (2017) 3363–3367.
[42] A. Karam, K. De Oliveira Vigier, S. Marinkovic, B. Estrine, C. Oldani, F. Jérôme, ChemSusChem 10 (2017) 3604–3610.
[43] Y. Dou, S. Zhou, C. Oldani, W. Fang, Q. Cao, Fuel 214 (2018) 45–54.
[44] M.C. Duclos, A. Herbinski, A.S. Mora, E. Métay, M. Lemaire, ChemSusChem 11 (2018) 547–551.
[45] V. Trombettoni, L. Bianchi, A. Zupanic, A. Porciello, M. Cuomo, O. Piermatti, A. Marrocchi, L. Vaccaro, Catalysts 7 (2017) 235–249.
[46] A. Karam, P.N. Amaniampong, J.M. García Fernández, C. Oldani, S. Marinkovic, B. Estrine, K. De Oliveira Vigier, F. Jérôme, Front. Chem. 6 (2018) 74.
[47] S. Andreoli, C. Oldani, V. Fiorini, S. Stagni, G. Fornasari, S. Albonetti, Appl. Catal. A Gen. 597 (2020), 117544.
[48] P. Barbaro, F. Liguori, C. Oldani, C. Moreno-Marrodán, Adv. Sustainable Syst. (2020), 1900117.
[49] M. Gilbert (Ed.), Brydson's Plastics Materials, 8th edition, Elsevier, Amsterdam, 2017.
[50] A. Rudin, P. Choi, The Elements of Polymer Science & Engineering, 3rd edition, Academic Press, Cambridge, 2013.
[51] A. Drelinkiewicz, A. Knapik, A. Waksmundzka-Góra, A. Bukowska, W. Bukowski, J. Noworól, React. Funct. Polym. 68 (2008) 1059–1071.
[52] G. Bernardo, D. Vesely, J. Appl. Polym. Sci. 115 (2010) 2402–2408.
[53] V. Arcella, A. Ghielmi, M. Apostolo, J. Abusleme (Ausimont S. p A.), Patent No. US0014405 (A1), 2002.
[54] L. Merlo, V.Tortelli, I. Wlassics, C. Oldani (Solvay Specialty Polymers Italy S.p. A.), Patent No. US9434679 (B2), 2016.
[55] M.T. Gokmen, F.E. Du Prez, Prog. Polym. Sci. 37 (2012) 365–405.
[56] G.V. Samsonov, V.A. Pasechnik, Russ. Chem. Rev. 38 (1969) 547–565.
[57] B. Corain, M. Zecca, K. Jeřábek, J. Mol. Catal. A Chem. 177 (2001) 3–20.
[58] R. Selke, K. Häupke, W. Krause, J. Mol. Catal. 56 (1989) 315–328.
[59] O. Okay, Prog. Polym. Sci. 25 (2000) 711–779.
[60] A. Rouocoux, J. Schulz, H. Patin, Chem. Rev. 102 (2002) 3757–3778.
[61] B. Corain, K. Jeřábek, P. Centomo, P. Canton, Angew. Chem. Int. Ed. 43 (2004) 959–962.
[62] H. Bönnemann, R.M. Richards, Eur. J. Inorg. Chem. (2001) 2455–2480.
[63] B. Corain, M. Zecca, P. Canton, P. Centomo, Philos. Trans. Math. Phys. Eng. Sci. 368 (2010) 1495–1507.
[64] V. Trombettoni, D. Lanari, P. Prinsen, R. Luque, A. Marrocchi, L. Vaccaro, Prog. Energ. Combust. Sci. 65 (2018) 136–162.
[65] The Dow Chemical Company, Form No. 177-02436-0511 (accessed May 2020).
[66] The Dow Chemical Company, Form No. 177-03100-0313 (accessed May 2020).
[67] A.J. Seen, J. Mol, Catal. A: Chemical 177 (2001) 105–112.
[68] M. Ahmed, M.A. Malik, S. Pervez, M. Raffiq, Eur. Polym. J. 4 (2004) 1609–1613.
[69] C. Moreno Marrodan, D. Berti, F. Liguori, P. Barbaro, Catal. Sci. Technol. 2 (2012) 2279–2290.
[70] K. Mc Eleney, C.M. Crudden, J.H. Horton, J. Phys. Chem. C 113 (2009) 1901–1907.
[71] M. Muniz-Miranda, S. Caporali, P. Marsili, E. Giorgetti, Mater. Chem. Phys. 167 (2015) 188–193.
[72] L. Ren, L. Yang, P. Yu, Y. Wang, L. Mao, ACS Appl. Mater. Interfaces 5 (2013) 11471. –1147.
[73] J. Bi, J. Chen, Y. Dong, W. Guo, D. Zhu, T. Li, J. Polym. Sci.: Polym. Chem. Ed. 56 (2018) 2344–2353.
[74] A. Biffis, H. Landes, K. Jeřábek, B. Corain, J. Mol. Catal. A Chem. 151 (2000) 283–288.
[75] W.K. O'Keefe, M. Jiang, F.T.T. Ng, G.L. Rempel, Chem. Eng. Sci. 60 (2005) 4131–4140.
[76] Y.Z. Chen, B.J. Liaw, H.R. Tan, K.L. Shen, Appl. Catal. A Gen. 205 (2001) 61–69.
[77] C.U. Pittman, Y.F. Liang, J. Org. Chem. 45 (1980) 5048–5052.
[78] F. Winter, A. J.van Dillen, K.P. de Jong, J. Mol. Catal. A Chem. 219 (2004) 273–281.
[79] S.C. Patankar, S.K. Dodiya, G.D. Yadav, J. Mol. Catal. A Chem. 409 (2015) 171–182.
[80] S. Talwalkar, S. Mahajani, Appl. Catal. A Gen. 302 (2006) 140–148.
[81] Z. Lei, J. Li, C. Li, B. Chen, Korean J. Chem. Eng. 23 (2006) 264–270.
[82] A.K. Teotia, H. Sami, A. Kumar, Thermo-responsive polymers: structure and design of smart materials. Switchable and Responsive Surfaces and Materials for Biomedical Applications, Elsevier, 2015, pp. 3–43, pages.
[83] M. Rubinstein, R.H. Colby, Polymer Physics, Oxford University Press, New York, 2003.
[84] See Supporting Information.
[85] C. Moreno-Marrodan, F. Liguori, P. Barbaro, Beilstein J. Org. Chem. 13 (2017) 734–754.
[86] F. Liguori, P. Barbaro, J. Catal. 311 (2014) 212–220.
[87] X. Kong, Y. Zhu, Z. Fang, J.A. Kozinski, I.S. Butler, L. Xu, H. Songa, X. Wei, Green Chem. 20 (2018) 3657–3682.
[88] D. Adu-Mensah, D. Mei, L. Zuo, Q. Zhang, J. Wang, Fuel 251 (2019) 660–668.
[89] R.M. Myers, D.E. Fitzpatrick, R.M. Turner, S.V. Ley, Chem. Eur. J. 20 (2014) 12348–12366.
[90] Á. Molnár, A. Papp, Coord. Chem. Rev. 349 (2017) 1–65.
[91] N.M. Prinsloo, J.P. Engelbrecht, T.N. Mashapa, M.J. Strauss, Appl. Catal. A Gen. 344 (2008) 20–29.
[92] R.D. Hetterley, E.F. Kozhevnikova, I.V. Kozhevnikov, Chem. Commun. (Camb.) (2006) 782–784.
[93] A.A. Nikolopoulos, B.W, L. Jang, J.J. Spivey, Appl. Catal. A Gen. 296 (2005) 128–136.
[94] Yi. Pan, B. Yuan, Y. Li, D. He, Chem. Commun. (Camb.) 46 (2010) 2280–2282.
[95] P. Wang, S. Bai, J. Zhao, P. Su, Q. Yang, Can Li, ChemSusChem 5 (2012) 2390–2396.
[96] R. Ma, Y. Li, G. Wu, Y. He, J. Feng, Y. Zhao, D. Li, Chinese J. Catal. 39 (2018) 1384–1394.
[97] E.F. Kozhevnikova, I.V. Kozhevnikov, J. Catal. 238 (2006) 286–292.
[98] J.I. Di Cosimo, G. Torres, C.R. Apesteguía, J. Catal. 208 (2002) 114–123.
[99] G. Torres, C.R. Apesteguía, J.I. Di Cosimo, Appl. Catal. A Gen. 317 (2007) 161–170.
[100] J.H. Clark, F. Deswarte, Introduction to Chemicals From Biomass, 2nd edition, Wiley, 2015.
[101] P. Sudarsanam, E. Peeters, E.V. Makshina, V.I. Parvulescu, B.F. Sels, Chem. Soc. Rev. 48 (2019) 2366–2421.
[102] G. Gómez Millán, S. Hellsten, J. Llorca, R. Luque, H. Sixta, A.M. Balu, ChemCatChem 11 (2019) 2022–2042.
[103] E. Ramírez, R. Bringué, C. Fité, M. Iborra, J. Tejero, F. Cunill, J. Chem. Technol. Biotechnol. 92 (2017) 2775–2786.